Comparison of Moderate Resolution Imaging Spectroradiometer ocean aerosol retrievals with ship-based Sun photometer measurements from the Around the Americas expedition

A. F. Adames,[1,2] M. Reynolds,[3] A. Smirnov,[4,5] D. S. Covert,[1,2] and T. P. Ackerman[1,2]

Received 4 December 2010; revised 12 May 2011; accepted 24 May 2011; published 19 August 2011.

[1] The Around the Americas expedition was a 25,000 mile sailing circumnavigation of the North and South American continents, in coastal waters, that took place from June 2009 to June 2010. The broad geographical span of the voyage made it possible to measure marine aerosol optical depths in regions where surface measurements are not frequently taken. These were measured with a handheld Microtops II Sun photometer. In this study we compare these measurements with the ocean aerosol product from the Moderate Resolution Imaging Spectroradiometer (MODIS) aboard the Aqua and Terra platforms. Results for aerosol optical depth (AOD) show a strong relationship between both measurements, with most values from MODIS falling within published expectations. However, MODIS values are biased high relative to surface observations for small optical depth values. There appears to be a relationship between these discrepancies in measurements and surface wind speed, with a group of values showing overestimation at wind speeds near and over 6 m/s and a second, smaller group showing underestimation for calmer conditions. For derived Ångström exponents, it is found that higher differences occur at low AOD. No relationship between these differences and wind speed is found.

Citation: Adames, A. F., M. Reynolds, A. Smirnov, D. S. Covert, and T. P. Ackerman (2011), Comparison of Moderate Resolution Imaging Spectroradiometer ocean aerosol retrievals with ship-based Sun photometer measurements from the Around the Americas expedition, *J. Geophys. Res.*, *116*, D16303, doi:10.1029/2010JD015440.

1. Introduction

[2] Aerosol particles are an important component of the global climate system. However, their composition, abundance and size distributions remain poorly understood [*Kinne et al.*, 2003]. Such diversity in particles, which come from natural as well as anthropogenic sources, results in large variations in aerosol optical depth (AOD) and absorptivity that lead to uncertainties in regional and global radiative forcing [*Haywood and Boucher*, 2000]. In order to further understand the impacts of aerosols in our climate system, many direct, surface-based measurement systems have been deployed, which include the Aerosol Robotic Network (AERONET) [*Holben et al.*, 1998] and the U.S. Department of Energy's Atmospheric Radiation Measurement (ARM) program [*Ackerman and Stokes*, 2003].

[3] Even though these networks are continuously taking AOD measurements at their fixed sites, they are almost always situated on land. Accurate sources of AOD information over the open ocean remain scarce, and more information is still needed to further understand the effects of particles on the environment [*Abdou et al.*, 2005]. The Maritime Aerosol Network (MAN) has been developed as a component of AERONET in order to gather aerosol information at sea by means of ship-based measurements [*Smirnov et al.*, 2009]. An opportunity to provide valuable information on oceanic aerosol properties arose with the Around the Americas (ATA) expedition. ATA was a 25,000 mile circumnavigation of the American coastlines (Figures 1a–1c) by sailboat, the S/V *Ocean Watch* (OW), arising from a partnership of Sailors of the Sea with Pacific Science Center in Seattle, WA [*Reynolds et al.*, 2010; *McCormick* 2010] (see http://www.sea-technology.com/features/2010/0810/around_the_americas.html). The broad geographical span of the voyage made it possible to measure oceanic aerosol properties in regions where measurements are not frequently taken. The expedition lasted from early June 2009 to late June 2010, during which aerosol properties were measured using a handheld Microtops II Sun photometer [*Morys et al.*, 2001].

[4] In this study we review the aerosol data obtained from the Microtops Sun photometer aboard the OW during the 13 month expedition and compare it with satellite derived properties of the standard aerosol product from the Moderate

[1]Joint Institute for the Study of the Atmosphere and Ocean, University of Washington, Seattle, Washington, USA.
[2]Also at Department of Atmospheric Sciences, University of Washington, Seattle, Washington, USA.
[3]Remote Research and Measurement Company LLC, Seattle, Washington, USA.
[4]NASA Goddard Space Flight Center, Greenbelt, Maryland, USA.
[5]Also at Sigma Space Corporation, Lanham, Maryland, USA.

0148-0227/11/2010JD015440

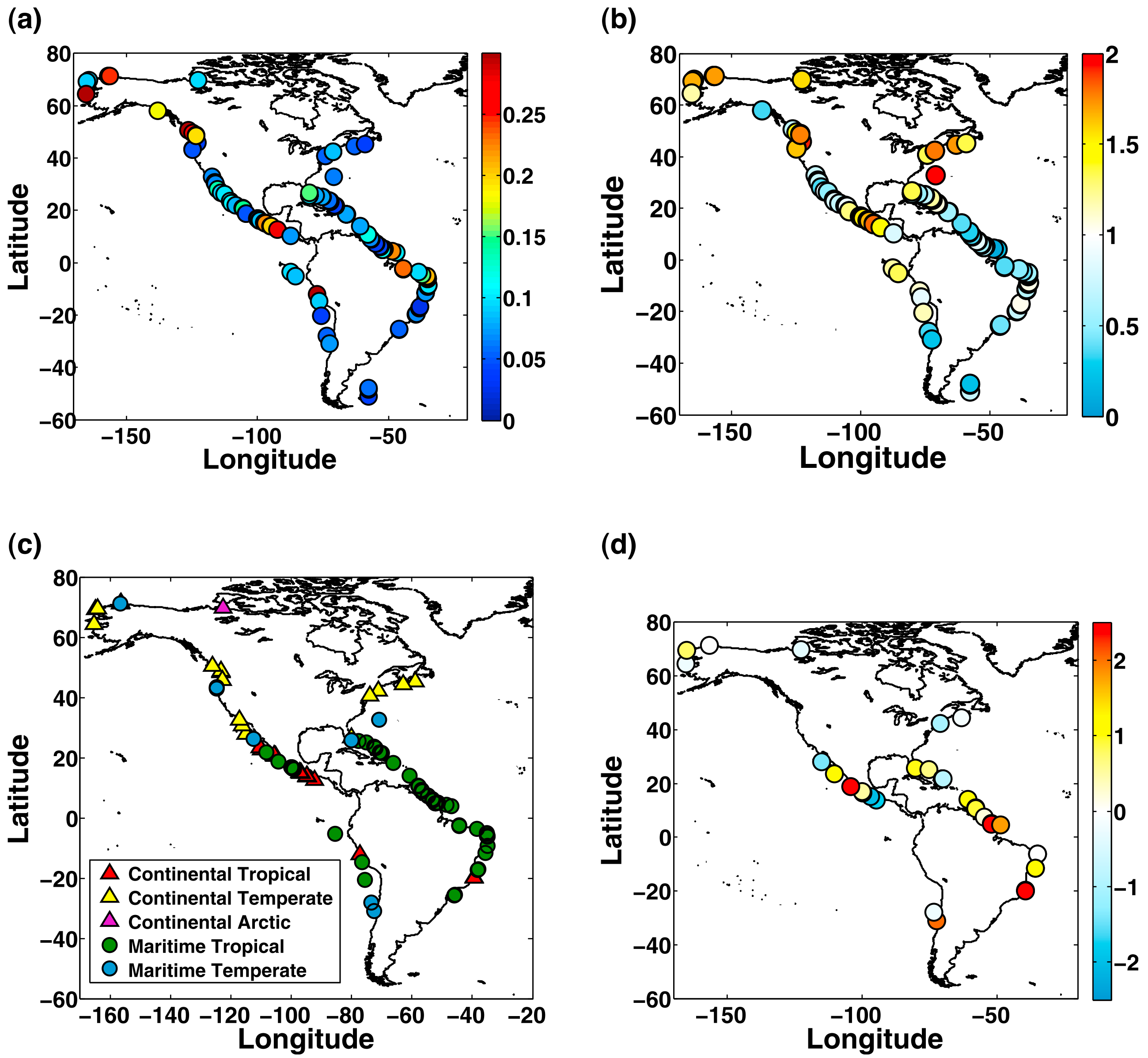

Figure 1. (a) Locations of available Microtops measurements from the *Ocean Watch*. The aerosol optical depth (AOD) value at $\lambda = 550$ nm is indicated by the color of the dot. The 550 nm value is obtained via log-log interpolation from the actual Microtops measurements. (b) Locations of measurements with the derived 440–870 nm Ångström exponent. (c) Air mass classifications for each measurement point. (d) Sites of colocated Microtops measurements with Moderate Resolution Imaging Spectroradiometer (MODIS)-retrieved aerosol products. The color bar denotes the expectation error between both sensors in the 550 nm band. An expectation error that is greater than ±1 means that the difference between measured AODs exceeds MODIS's estimated uncertainty interval. Because some observations are closely located in space, some points are hidden.

Resolution Imaging Spectroradiometer (MODIS) [*Kaufman et al.*, 1997a].

2. Microtops Data

[5] Manufactured by Solar Light Co. Inc. (Philadelphia, Pennsylvania), the Microtops II Sun photometer is a compact, lightweight, portable instrument [*Morys et al.*, 2001]. It measures solar radiance at four channels (380, 440, 675 and 870 nm) from which it derives its corresponding aerosol optical depth (AOD). The filters used for each channel have a peak wavelength precision of ±1.5 nm and a full width at half maximum band-pass of 10 nm (http://www.solarlight.com/products/sunphoto.html).

2.1. Calibration and Data Quality

[6] The instrument was calibrated prior to deployment by comparison with a reference AERONET Sun photometer located at NASA Goddard Space Flight Center. Uncertainties in Microtops AOD measurements at sea are largely due to

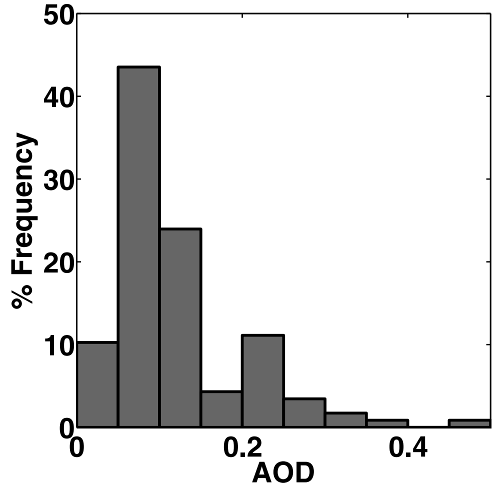

Figure 2. Frequency distribution of all AOD measurements (λ = 550 nm) taken during Around the Americas (ATA).

calibration. Previous studies estimate errors to be in the range of plus or minus 0.02 [*Knobelspiesse et al.*, 2004; *Ichoku et al.*, 2002b].

[7] In order to minimize aiming and cloud contamination errors, multiple Sun photometer measurements were taken during each observation; higher values obtained via this procedure are discarded, because smaller values correspond to the most accurate Sun pointing [*Porter et al.*, 2001]. To avoid any possible cloud contamination, measurements were only done on clear days, with few or no clouds covering the sky, particularly at angles close to the Sun. The final product comprises level 2.0 data in which values are postcalibrated, cloud and pointing error screened, and quality assured [*Smirnov et al.*, 2000a, 2009].

2.2. ATA Measurements

[8] A total of 699 AOD measurement scans were made during the ATA. A measurement scan involved standing in an exposed area on the OW deck and holding the instrument toward the Sun to an accuracy of ±2° approximately. A single scan takes 20 s during which approximately 32 analog-to-digital samples of the photo cells are made. The Microtops was programmed to accept only the maximum voltage sample of the entire scan, which corresponds to the minimum optical depth. The complete database of measurements from ATA is available in the Maritime Aerosol Network database [*Smirnov et al.*, 2009] (http://aeronet.gsfc.nasa.gov/new_web/cruises_new/Around_the_Americas.html). Each observation group, comprising 1–20 measurements within a time range of 10 min or less, was averaged. However, only observations that contained at least two measurements, with data points being no more than 20% apart for these cases, were used. This criterion is applied to avoid any overestimation from the Microtops that might be due to ship movement, or cloud contaminated cases that might have passed through screening. The standard deviation for each group was also derived. The resulting data set, which is used in this study, comprises 117 observations spread over a wide geographical area (Figure 1). The 550 nm AOD as well as the 440–870 nm Ångström exponent values obtained for this data set are shown in Figures 1a–1b. The frequency distribution (Figure 2) shows that 78% of these AOD values are less than 0.15, indicating the dominance of low aerosol loadings during the expedition. This distribution is similar to that obtained by *Smirnov et al.* [2011].

2.3. Comparison With Data From Barrow, Alaska

[9] In mid 2009, the OW made four observations during different days in port at Pt. Barrow, Alaska. An opportunity arose to investigate the quality of the Microtops measurements by comparing them to measurements from three instruments colocated at the ARM research facility in Barrow, AK, approximately 28 km away. The instruments are a Cimel Sun photometer [*Holben et al.*, 1998], a Multifilter Rotating Shadow Band Radiometer (MFRSR) [*Harrison et al.*, 1994] and a Normal Incidence Multifilter Radiometer (NIMFR) [*Michalsky et al.*, 2006]. Cimel Sun photometers are the primary radiometers utilized by AERONET. They measure direct Sun, aureole and sky radiances at a 1.2 full angle field of view [*Holben et al.*, 1998]. The MFRSR uses independent interference-filter-photodiode detectors and an automated rotating shadow band technique to make measurements of the diffuse and total solar flux, which are then differenced to obtain the direct solar flux [*Harrison et al.*, 1994]. The NIMFR is a modified MFRSR that looks directly at the Sun with a 5.7° field of view [*Michalsky et al.*, 2006]. Thus, all three instruments make measurements of the direct solar flux which is then used to determine the AOD.

[10] The average values of measurements within a 10 min period for all four instruments are compared. They are found to be within an expected accuracy of ±0.025 for 3 out of 4 days. On 17 July, the observed differences for the instruments ranged from 0.015 to 0.035 (Figure 3), for reasons that are unclear. A comparison of the three ARM instruments over a 70 day period, beginning on 1 June (Figure 4), shows that about 7%–14% of the observed differences in AOD are greater than 0.02, the expected calibration accuracy [*Holben et al.*, 1998; *Alexandrov et al.*, 2008; *Michalsky et al.*, 2006]. The MFRSR experienced some shadow band alignment problems while the NIMFR also showed functional problems during parts of this period. Both the MFRSR and the NIMFR measurements are posi-

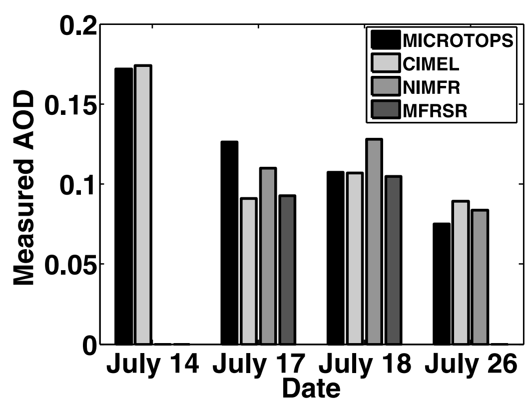

Figure 3. Comparison of Microtops measurements with three instruments located at the atmospheric radiation measurement site in Barrow, Alaska, for the 4 days during which Microtops measurements were made (λ = 675 nm).

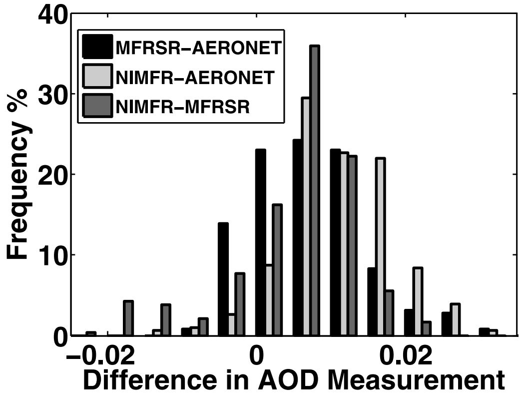

Figure 4. Frequency distribution of the difference of measured AOD (λ = 500 nm) for the three instruments located at Barrow, Alaska, for a 70 day time period beginning on 1 June 2009.

tively biased when compared to the Cimel. However, even if we disregard these measurements, differences larger than 0.02 are still possible (Figure 3). Accounting for this error and for pointing difficulties due to ship movement, we set the uncertainty for the ATA Microtops measurements at 0.025, as was indicated by *Porter et al.* [2001].

2.4. Analysis of Synoptic Air Masses

[11] Microtops data was additionally classified according to regional characteristics. Classifications follow a traditional method that assumes the existence of an arctic front and a polar front. Thus, air masses can be classified into arctic, polar and tropical, being additionally either marine or continental [*Smirnov et al.*, 1995]. In this study, we also divide data into four oceanic regions: north and south Atlantic, and north and south Pacific. Classification was done mainly using the Hybrid Single-Particle Lagrangian Integrated Trajectory (HYSPLIT) (http://ready.arl.noaa.gov/ ; see also http://ready.arl.noaa.gov/HYSPLIT.php) model back trajectories for a time period of 72 h (Figure 5). Trajectories that passed over major landmasses during this period, or had a source attribution to landmasses are classified as continental while those that did not are classified as maritime. An exception to this classification scheme would be if the trajectory followed a track over a generally unpolluted area with little to no sources of aerosols (i.e., Greenland) [*Smirnov et al.*, 1995]. The arctic, polar or tropical classification is labeled according to the source location of the back trajectory. Meteorological maps from NOAA's Tropical Analysis and Forecast Branch analysis were used, when available, to aid in classification. Examples of classifications with this scheme are shown in Figure 5.

[12] A summary of results obtained is presented in Table 1 while the classification for each measurement is shown in Figure 1c. Results from this classification show a dominance of marine tropical air for ATA, with 58% of all measurements falling into this category. Optical depths in this category were mostly low, with values falling mostly between 0.06 and 0.08 with a relatively high standard deviation that ranges from 0.02 to 0.04. The outlying case is the South Atlantic, in which high optical depth values were observed. This case is likely due to the presence of Saharan dust and/or biomass-burning aerosols, which are characterized by having high optical depths and low Ångström exponent values. These results were also observed during the Aerosol99 experiment in this region [*Voss et al.*, 2001], with the highest measured AODs in this region comparable to those found in that study. Derived values for Ångström exponents for maritime tropical air are in the range of 0.65 for the whole Atlantic. Mean values for Ångströms are found to be much larger in the Pacific, ranging from 1.12 to 1.39, meaning a stronger presence of fine mode aerosols. This differs significantly from values obtained by *Smirnov et al.* [1995]. Continental tropical air masses, in particular those in the north Pacific (off the coast of Central America and Mexico) have much higher AOD values, which might be indicative of more recent air pollution. Results for temperate (polar) air masses show higher values for AOD for continental sources, particularly in the north Pacific. AOD results for maritime polar air in the north Atlantic is close to those found by *Voss et al.* [2001] and *Smirnov et al.* [2000b], but values for derived Ångström exponents in this study are found to be somewhat higher. This might be due to higher uncertainties in the derivation due to low AOD as well as the presence of remaining pollutants in the area. Some of the other classifications cannot be comprehensively evaluated due to the small amount of data samples in those groups.

3. MODIS Data

[13] The Moderate Resolution Imaging Spectroradiomenter (MODIS) is an instrument aboard the Earth Observing System Aqua and Terra satellites [*Salomonson et al.*, 1989]. Measurements from MODIS are performed in 36 channels spanning the visible and infrared regions at a spatial resolution of 250 m, 500 m, or 1 km, depending on wavelength [*Barnes et al.*, 1998]. The two instruments provide nearly global coverage daily. Because of its wide spectral range, broad swath and fine spatial resolution, MODIS has become a highly used source for information on aerosol optical properties.

[14] The MODIS standard aerosol algorithm comprises two different and independent algorithms. Their products are currently organized and reprocessed in collection 051. The first algorithm derives aerosol properties over land [*Kaufman et al.*, 1997b; *Remer et al.*, 2005; *Levy et al.*, 2007], and the second over ocean [*Tanré et al.*, 1997; *Levy et al.*, 2003; *Remer et al.*, 2005]. The ocean algorithm masks out clouds, suspended river sediments and solar glint, which affect the quality of retrieved data [*Martins et al.*, 2002; *Li et al.*, 2003; *Levy et al.*, 2003], and retrieves aerosol properties at seven wavelengths (470, 550, 660, 870, 1240, 1630, and 2130 nm). *Remer et al.* [2005] have shown that the ocean algorithm gives an optical depth accuracy of $\Delta\tau = \pm (0.03 + 0.05\tau)$, where τ is the AOD at a particular wavelength (λ). The most recent document describing the MODIS algorithm, "Algorithm for Remote Sensing of Tropospheric Aerosol Over Dark Targets From MODIS," is available at http://modis-atmos.gsfc.nasa.gov/_docs/ATBD_MOD04_C005_rev2.pdf.

4. Comparison of MODIS Retrievals With Microtops

[15] In order to compare Microtops measurements with data from MODIS's overpasses of OW, we incorporated a

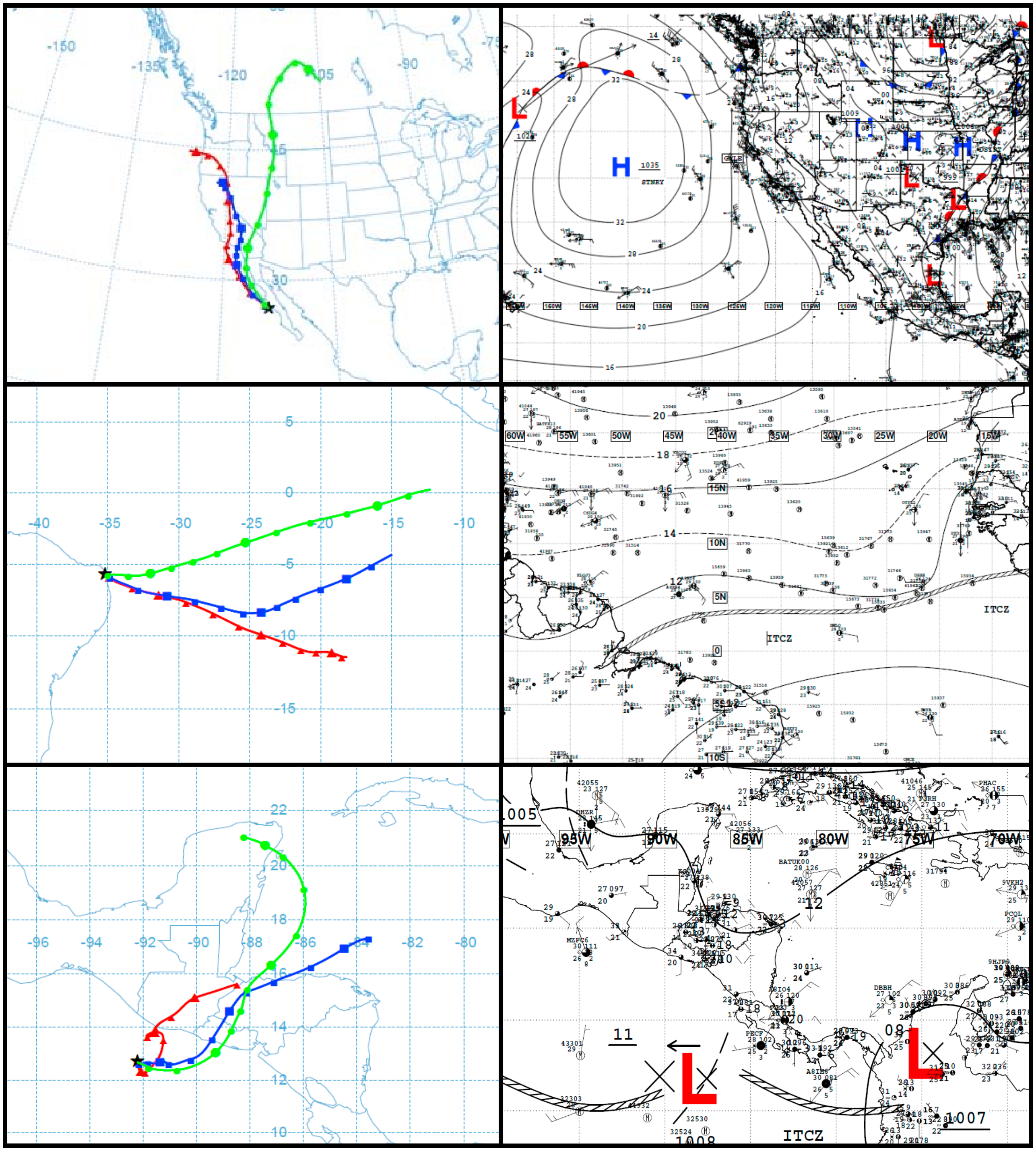

Figure 5. Sample HYSPLIT back trajectories at 500 m (red), 1000 m (blue), and 3000 m (green), along with Tropical Analysis and Forecast Branch analysis products showing the atmospheric conditions for (top) continental polar (temperate), (middle) maritime tropical, and (bottom) continental tropical samples for three measurements obtained during ATA. H and L denote high- and low-pressure systems.

spatiotemporal approach similar to that of *Ichoku et al.* [2002a]. Because we expect that AOD over ocean does not vary much on spatial scales of a few hundred kilometers [*Smirnov et al.*, 2002; *Anderson et al.*, 2003], and because measurements were only taken on essentially cloudless days, the time difference between Sun photometer measurement and MODIS overpass was set to ±90 min. This is generous when compared to the 60 min Sun photometer data segment protocol proposed by *Ichoku et al.* [2002a]. MODIS aerosol retrievals were averaged over a 50 × 50 km^2 area around the Sun photometer site. Only retrievals that contained data in at least five pixels (20% of measured area)

Table 1. Mean Aerosol Optical Depths and Ångström Exponents for the Synoptic Air Masses Encountered During ATA[a]

Air Mass Type	Location	$\tau_{550} \pm \sigma_\tau$	Median τ_{550}	$\alpha \pm \sigma_\alpha$	Median α	N
			Continental			
Tropical	N. Pacific	0.18 ± 0.06	0.19	1.36 ± 0.39	1.54	12
	S. Pacific	0.30	0.30	1.11	1.11	1
	S. Atlantic	0.07	0.07	0.77	0.77	2
Polar	N. Pacific	0.17 ± 0.12	0.14	1.38 ± 0.56	1.68	13
	N. Atlantic	0.08 ± 0.05	0.06	1.58 ± 0.25	1.49	10
Arctic	N. Pacific	0.14	0.15	1.41	1.57	3
			Maritime			
Tropical	N. Pacific	0.07 ± 0.02	0.07	1.39 ± 0.29	1.47	9
	S. Pacific	0.07	0.09	1.12	1.16	3
	N. Atlantic	0.08 ± 0.04	0.07	0.65 ± 0.38	0.54	37
	S. Atlantic	0.13 ± v0.08	0.11	0.65 ± 0.30	0.57	18
Polar	N. Pacific	0.08	0.08	1.36	1.60	4
	S. Pacific	0.06	0.06	0.29	0.29	2
	N. Atlantic	0.09	0.10	0.78	0.58	3

[a]Here τ_{550} is the aerosol optical depth at 550 nm (interpolated), σ_τ is the standard deviation for optical depth, α is the Ångström exponent, σ_α is the standard deviation for the Ångström exponent, and N is the number of analyzed measurements. Median values for τ_{550} and α are also included. Standard deviation is only included for those groups that contain five or more measurements.

were used. The result is a total of 35 cases in which MODIS retrievals can be compared with ATA Microtops measurements. We investigated the impact of incorporating tighter time constraints, which resulted in a data set of only 17 points, but there were no significant differences between the 17-point and 35-point data sets.

[16] Because MODIS and Microtops make measurements at different wavelengths, AOD values were matched using a log-log Ångström relation between AOD and wavelength [*Eck et al.*, 1999]. All of the Aqua observations in this study were reprocessed in collection 051 (http://modisatmos.gsfc.nasa.gov/_docs/ATBD_MOD04_C005_rev2.pdf) while Terra data were reprocessed in collection 005 (http://modis-atmos.gsfc.nasa.gov/_docs/MOD04:MYD04_ATBD_C005_rev1.pdf) until 15 April 2010, when it switched to 051. While some changes were made in the new collection (http://modis-atmos.gsfc.nasa.gov/_docs/Collection_051_Changes_v1.pdf), these have a minimal effect on results obtained in this study. In addition to the criteria applied to match MODIS and Microtops data, some additional data loss occurred when the OW was located within or near the solar glint. Locations where comparisons occurred are shown in Figure 1d.

4.1. Aerosol Optical Depth

[17] A scatterplot of the spatiotemporal comparison between MODIS AOD and Microtops AOD is shown in Figure 6. The 1:1 line is denoted by a purple dashed line while the purple dotted lines represent the boundaries of uncertainty defined by *Remer et al.* [2005] as $\Delta\tau = \pm (0.03 + 0.05\tau)$. Around 61% of measurements fall within these boundaries, which is in good agreement with previous reports [*Levy et al.*, 2005; *Remer et al.*, 2008]. The averaged AOD for the MODIS 550 nm channel gives a result of 0.13, which is similar to the global marine AOD results found by *Remer et al.* [2008] (0.13 for Aqua-MODIS and 0.14 for Terra-MODIS), and slightly larger than the averaged Microtops AOD at the same wavelength (AOD = 0.12). A linear regression for each of the three wavelengths is also plotted. These lines have slopes very close to one and high correlation coefficients, indicative of a strong linear relationship between both measurements. However, a significant number of values are observed to lie above the uncertainty estimates, all occurring at low optical depths (AOD < 0.15). These points comprise 34% of all measured values at clean conditions. There is no observed geographical distribution of this group (Figure 1d). It is known that MODIS retrievals are less accurate at low AOD due to noise sources, such as surface reflectance, boundary conditions

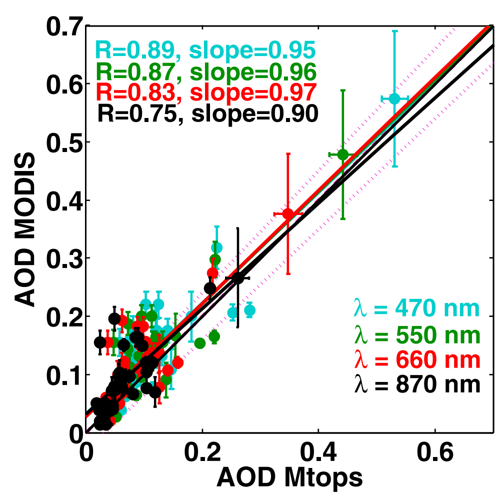

Figure 6. Scatterplot of MODIS against Sun photometer aerosol optical depth measured during ATA for four wavelengths, with their respective regression lines. The two purple dotted lines denote the expectation error boundaries for MODIS, while the middle purple dashed line represents the 1:1 line. The vertical error bars represent spatial standard deviation from MODIS AOD retrievals within the 50 km box, while the horizontal error bars are temporal standard deviations from Microtops.

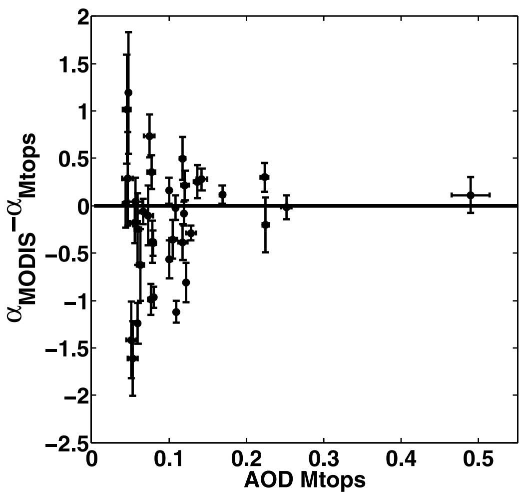

Figure 7. Difference between MODIS 550–870 nm Ångström exponent and Microtops derived Ångström exponent as a function of Microtops optical depth at 550 nm. Vertical error bars denote the error propagation of the difference between uncertainties in measurements from both instruments, while the horizontal error bars are the standard deviation for the Microtops measurements.

and particle properties [*Chu et al.*, 2005; *Levy et al.*, 2005; *Zhang and Reid*, 2006; *Kahn et al.*, 2007], but our data show that the MODIS values are biased high relative to surface observations for small optical depth values.

4.2. Ångström Exponent

[18] The Ångström exponent is a measure of the spectral dependence of the aerosol extinction coefficient and is, consequently, a qualitative indicator of aerosol particle size [*Ångström*, 1929; *Schuster et al.*, 2006]. Since the Ångström exponent is known to vary with wavelength [*King and Byrne*, 1976; *Eck et al.*, 1999], we calculate the Ångström exponent from the Microtops data measurements using the equation defined by *Remer et al.* [2005] as

$$\alpha = -\ln(\tau\lambda_1/\tau\lambda_2)/\ln(\lambda_1/\lambda_2), \qquad (1)$$

where $\tau_{\lambda1}$ and $\tau_{\lambda2}$ are the AODs for each wavelength, λ_1 = 550 nm and λ_2 = 870 nm, respectively. A scatterplot comparing Ångström exponents shows no distinguishable relationship between the two measurements. The difference between α values from MODIS and from the Microtops measurements plotted as a function of optical depth (Figure 7) shows larger discrepancies at lower AOD values. This discrepancy is presumably due to the higher relative uncertainty in AOD measurements from both the Sun photometer and MODIS in cleaner conditions. While these errors are not as significant in optical depth measurements, they are amplified and create larger uncertainties when the Ångström exponent is calculated [*Ignatov et al.*, 1998]. The Ångström coefficients compare much better at higher aerosol loadings (AOD $\geq$ 0.15).

4.3. Wind Speed Analysis

[19] *Zhang and Reid* [2006] discuss major sources of bias produced in the MODIS aerosol ocean product from cloud contamination, aerosol microphysical properties and lower boundary conditions. At low AOD, these uncertainties can significantly alter AOD values. One of the major sources of uncertainty in lower boundary conditions is from the near-surface wind field [*Zhang and Reid*, 2006]. Here we compare the derived aerosol properties with wind speed measurements made by a Vaisala Weather Transmitter WXT520 aboard OW. The instrument takes measurements every two minutes with an estimated precision of ±0.3 m/s (manufacturer's specification). The wind speed measurement reported here is an average of measurements at an interval of ±20 min surrounding MODIS observations. The chosen time interval gives a reasonable value of average wind speed inside the box region while averaging out biases that might occur due to gusts or lulls and measurement uncertainties.

[20] The expectation error is used to quantify the magnitude of the difference in AOD from both sensors in relation to the uncertainty estimates defined by *Remer et al.* [2002]. This quantity describes the difference between MODIS and Microtops AODs with respect to MODIS's estimated uncertainty boundaries of $\pm(0.03 + 0.05\tau)$. It was defined by *Levy et al.* [2003] as

$$\tau_{\mathrm{ExpErr}} = (\tau_{\mathrm{MODIS}} - \tau_{\mathrm{Mtop}})/(0.03 + 0.05\tau_{\mathrm{Mtop}}), \qquad (2)$$

where τ_{MODIS} is the AOD measurement from MODIS and τ_{Mtop} is the measurement from the Microtops Sun photometer. A value for the expectation error whose magnitude is greater than one means that the difference between measured AODs exceeds MODIS's estimated uncertainty interval. Moreover, a value between ±1 means that the observed differences are within MODIS's expected uncertainty. The correlation between the expectation error at all four wavelengths and the measured wind speed is shown in Figure 8a. Even though a regression analysis does not show a strong relationship in these values, the plot shows that measurements can be divided in two groups: one group with a positive expectation error at average winds speeds near and above 6 m/s, and a second, smaller group with a negative expectation error for average wind speeds below 6 m/s. This result is almost identical for all wavelengths. A plot of Microtops measured optical depth versus wind speed (Figure 8b) shows no significant relationship between Sun photometer measured optical depth and the prevailing winds for the compared cases. On the other hand, a stronger relationship is found for AOD values in maritime tropical environments when there is no dust or biomass-burning aerosols present (Figure 8c). This group, comprising 44 measurements, shows a regression slope (λ = 550 nm) that agrees well with results obtained by *Smirnov et al.* [2003] and *Shinozuka et al.* [2004]. This increment in AOD is due to increased production of sea salt aerosols [*Quinn et al.*, 1998; *Shinozuka et al.*, 2004], which can be measured when unpolluted conditions prevail. This result might be suggestive that, while sea salt aerosol particles contribute to an increased AOD in high-wind conditions, it does not

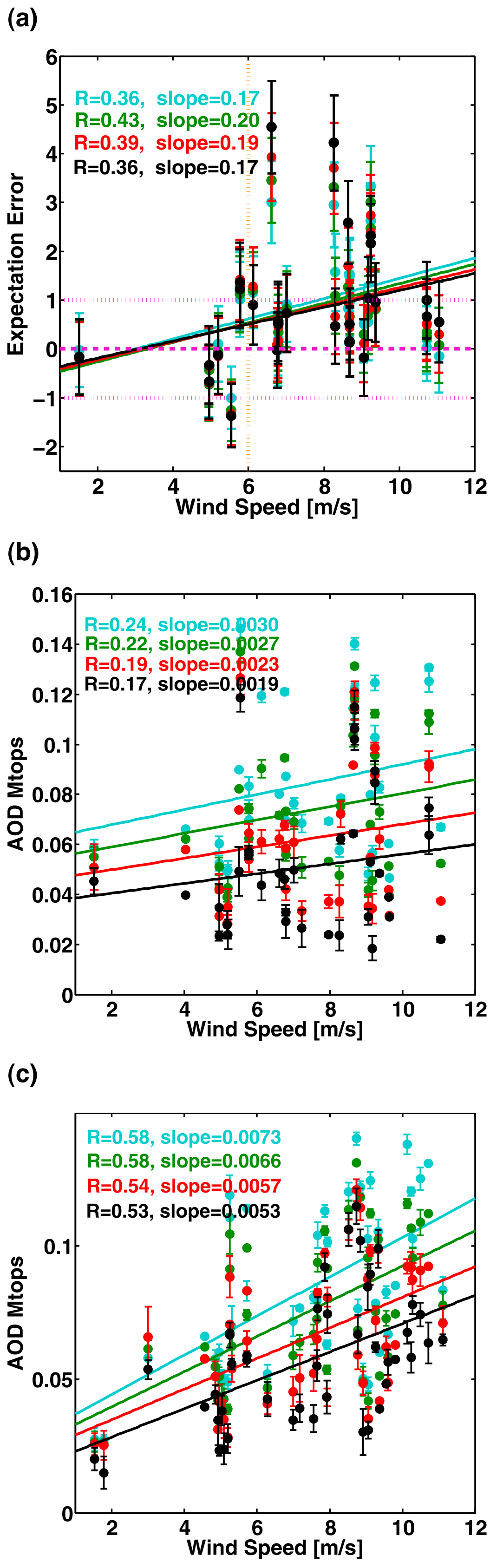

Figure 8. (a) Expectation error at four wavelengths as a function of average wind speed for Microtops AODs lower than 0.15. An expectation error that is greater than ±1 means that the difference between AODs exceeds MODIS's estimated uncertainty interval. The solid lines represent the linear fits, dotted lines represent the uncertainty boundaries defined by $\Delta\tau = \pm(0.03 + 0.05\tau)$, and the dashed line denotes a perfect AOD retrieval. The vertical dotted line indicates a value of 6 m/s, which is used in the MODIS standard algorithm. Horizontal error bars are the standard deviation of measured wind speed. (b) Microtops-measured AOD as a function of wind speed for the observations that were compared with MODIS (AOD < 0.15), and (c) Microtops-measured AOD as a function of average wind speed for cases classified as marine tropical with AOD < 0.15.

explain the observed bias in MODIS for such cases. A similar procedure was attempted for differences between derived Ångström exponents and wind speed, but no correlation was observed.

5. Summary

[21] For the ATA expedition a total of 117 observations were made aboard the OW research vessel. Low AOD values predominate, indicating low aerosol loadings at sea, even in the coastal regions. The frequency distribution of AOD values obtained during ATA is generally consistent with statistics from other MAN data sets [*Smirnov et al.*, 2011].

[22] We compare MODIS aerosol retrievals over the oceans with optical depth and Ångström exponent measurements from a Microtops Sun photometer. In general, AOD values from both instruments are in good agreement, with values falling mostly within previously published estimates. However, MODIS overestimates AOD compared to Microtops at low AOD values. Our results suggest a relationship between the differences in AOD measurements and surface wind speed. Thus, a possible reason for this discrepancy is MODIS's assumption that the surface wind speed is constant at 6 m/s [*Levy et al.*, 2003] (see also http://modisatmos.gsfc.nasa.gov/_docs/ATBD_MOD04_C005_rev2.pdf). This assumption may lead to MODIS underestimating the ocean surface contribution to measured radiation in zones where higher wind speeds prevail, because of surface wind expanding the solar glint region as well as higher production of white foams [*Zhang et al.*, 2005; *Moore et al.*, 2000]. The opposite may then be true for lower wind speed cases. Such an effect is unlikely to greatly affect MODIS's derived Ångström exponent, and trends in differences for Ångström exponent values due to wind speed are not seen in this study. However, most of the measurements compared were low optical depth cases, which produce higher uncertainties in Ångström exponent values for both sensors. These results are in good agreement with findings from *Zhang and Reid* [2006] and *Kahn et al.* [2007], which were based on AERONET measurements taken from islands and coastal regions, rather than the open ocean measurements reported here. Because of the prevalence of low optical depth values in oceanic regions, the sensitivity in MODIS's ocean algorithm to surface wind speed may result in an overestimation of aerosol optical depth

over the ocean, which in turn has implications for estimations of global aerosol loading, aerosol transport and concentration, and direct radiative forcing. Our small measurement sample demonstrates the need for additional surface measurements of aerosol properties over the world's oceans, particularly in remote regions where few measurements currently exist (see *Smirnov et al.* [2009] for a compilation of existing maritime measurements).

[23] **Acknowledgments.** This research is funded by the Joint Institute for the Study of the Atmosphere and Ocean (JISAO) under NOAA cooperative agreement NA17RJ1232. The crew of *Ocean Watch* supported this work with enthusiasm. In particular, David Logan and David Thoreson took measurements when at-sea scientists were not available.

References

Abdou, W. A., D. J. Diner, J. V. Martonchik, C. J. Bruegge, R. A. Kahn, B. J. Gaitley, K. A. Crean, L. A. Remer, and B. Holben (2005), Comparison of coincident Multiangle Imaging Spectroradiometer and Moderate Resolution Imaging Spectroradiometer aerosol optical depths over land and ocean scenes containing Aerosol Robotic Network sites, *J. Geophys. Res.*, *110*, D10S07, doi:10.1029/2004JD004693.

Ackerman, T. P., and G. Stokes (2003), The Atmospheric Radiation Measurement Program, *Phys. Today*, *56*, 38–45, doi:10.1063/1.1554135.

Alexandrov, M. D., A. A. Lacis, B. E. Carlson, and B. Cairns (2008), Characterization of atmospheric aerosols using MFRSR measurements, *J. Geophys. Res.*, *113*, D08204, doi:10.1029/2007JD009388.

Anderson, T. L., R. L. Charlson, D. M. Winker, J. A. Ogren, and K. Holmen (2003), Mesoscale variations of tropospheric aerosols, *J. Atmos. Sci.*, *60*, 119–136, doi:10.1175/1520-0469(2003)060<0119:MVOTA>2.0.CO;2.

Ångström, A. (1929), On the atmospheric transmission of Sun radiation and on dust in the air, *Geogr. Ann.*, *11*, 156–166, doi:10.2307/519399.

Barnes, W. L., T. S. Pagano, and V. V. Salomonson (1998), Prelaunch characteristics of the Moderate Resolution Imaging Spectroradiometer (MODIS) on EOS-AM1, *IEEE Trans. Geosci. Remote Sens.*, *36*, 1088–1100, doi:10.1109/36.700993.

Chu, D. A., et al. (2005), Evaluation of aerosol properties over ocean from Moderate Resolution Imaging Spectroradiometer (MODIS) during ACE-Asia, *J. Geophys. Res.*, *110*, D07308, doi:10.1029/2004JD005208.

Eck, T. F., B. N. Holben, J. S. Reid, O. Dubovik, A. Smirnov, N. T. O'Neill, I. Slutsker, and S. Kinne (1999), Wavelength dependence of the optical depth of biomass burning, urban, and desert dust aerosols, *J. Geophys. Res.*, *104*, 31,333–31,349, doi:10.1029/1999JD900923.

Harrison, L., J. J. Michalsky, and J. Berndt (1994), Automated multifilter rotating shadow-band radiometer: An instrument for optical depth and radiation measurements, *Appl. Opt.*, *33*, 5118–5125, doi:10.1364/AO.33.005118.

Haywood, J., and O. Boucher (2000), Estimates of the direct and indirect radiative forcing due to tropospheric aerosols: A review, *Rev. Geophys.*, *38*, 513–543, doi:10.1029/1999RG000078.

Holben, B. N., et al. (1998), AERONET—A federated instrument network and data archive for aerosol characterization, *Remote Sens. Environ.*, *66*, 1–16, doi:10.1016/S0034-4257(98)00031-5.

Ichoku, C., D. A. Chu, S. Mattoo, Y. J. Kaufman, L. A. Remer, D. Tanré, I. Slutsker, and B. N. Holben (2002a), A spatio-temporal approach for global validation and analysis of MODIS aerosol products, *Geophys. Res. Lett.*, *29*(12), 8006, doi:10.1029/2001GL013206.

Ichoku, C., et al. (2002b), Analysis of the performance characteristics of the five-channel Microtops II Sun photometer for measuring aerosol optical thickness and precipitable water vapor, *J. Geophys. Res.*, *107*(D13), 4179, doi:10.1029/2001JD001302.

Ignatov, A., L. Stowe, and R. Singh (1998), Sensitivity study of the Ångström exponent derived from AVHRR over oceans, *Adv. Space Res.*, *21*, 439–442, doi:10.1016/S0273-1177(97)00926-5.

Kahn, R. A., M. J. Garay, D. L. Nelson, K. K. Yau, M. A. Bull, B. J. Gaitley, J. V. Martonchik, and R. C. Levy (2007), Satellite-derived aerosol optical depth over dark water from MISR and MODIS: Comparisons with AERONET and implications for climatological studies, *J. Geophys. Res.*, *112*, D18205, doi:10.1029/2006JD008175.

Kaufman, Y., D. Tanré, H. Gordon, T. Nakajima, J. Lenoble, R. Frouin, H. Grassl, B. Herman, M. King, and P. Teillet (1997a), Passive remote sensing of tropospheric aerosol and atmospheric correction for the aerosol effect, *J. Geophys. Res.*, *102*, 16,815–16,830, doi:10.1029/97JD01496.

Kaufman, Y., D. Tanre, L. A. Remer, E. F. Vermote, A. Chu, and B. N. Holben (1997b), Operational remote sensing of tropospheric aerosol over land from EOS moderate resolution imaging spectroradiometer, *J. Geophys. Res.*, *102*, 17,051–17,067, doi:10.1029/96JD03988.

King, M., and D. Byrne (1976), A method for inferring total ozone content from the spectral variation of total optical depth obtained with a solar radiometer, *J. Atmos. Sci.*, *33*, 2242–2251, doi:10.1175/1520-0469(1976)033<2242:AMFITO>2.0.CO;2.

Kinne, S., et al. (2003), Monthly averages of aerosol properties: A global comparison among models, satellite data, and AERONET ground data, *J. Geophys. Res.*, *108*(D20), 4634, doi:10.1029/2001JD001253.

Knobelspiesse, K. D., C. Pietras, G. S. Fargion, M. H. Wang, R. Frouin, M. A. Miller, S. Subramaniam, and W. M. Balch (2004), Maritime aerosol optical thickness measured by handheld sunphotometers, *Remote Sens. Environ.*, *93*, 87–106, doi:10.1016/j.rse.2004.06.018.

Levy, R. C., L. A. Remer, D. Tanre, Y. J. Kaufman, C. Ichoku, B. N. Holben, J. M. Livingston, P. B. Russell, and H. Maring (2003), Evaluation of the Moderate-Resolution Imaging Spectroradiometer (MODIS) retrievals of dust aerosol over the ocean during PRIDE, *J. Geophys. Res.*, *108*(D19), 8594, doi:10.1029/2002JD002460.

Levy, R. C., L. A. Remer, J. V. Martins, Y. J. Kaufman, A. Plana-Fattori, J. Redemann, P. B. Russell, and B. Wenny (2005), Evaluation of the MODIS aerosol retrievals over ocean and land during CLAMS, *J. Atmos. Sci.*, *62*, 974–992, doi:10.1175/JAS3391.1.

Levy, R. C., L. A. Remer, S. Mattoo, E. F. Vermote, and Y. J. Kaufman (2007), Second-generation operational algorithm: Retrieval of aerosol properties over land from inversion of Moderate Resolution Imaging Spectroradiometer spectral reflectance, *J. Geophys. Res.*, *112*, D13211, doi:10.1029/2006JD007811.

Li, R.-R., Y. J. Kaufman, B.-C. Gao, and C. O. Davis (2003), Remote sensing of suspended sediments and shallow coastal waters, *IEEE Trans. Geosci. Remote Sens.*, *41*, 559–566, doi:10.1109/TGRS.2003.810227.

Martins, J. V., D. Tanré, L. Remer, Y. Kaufman, S. Mattoo, and R. Levy (2002), MODIS cloud screening for remote sensing of aerosols over oceans using spatial variability, *Geophys. Res. Lett.*, *29*(12), 8009, doi:10.1029/2001GL013252.

McCormick, H. (2010), Closing the circle, *Cruising World*, November 9, 50–55.

Michalsky, J. J., G. P. Anderson, J. Barnard, J. Delamere, C. Gueymard, S. Kato, P. Kiedron, A. McComiskey, and P. Ricchiazzi (2006), Shortwave radiative closure studies for clear skies during the Atmospheric Radiation Measurement 2003 Aerosol Intensive Observation Period, *J. Geophys. Res.*, *111*, D14S90, doi:10.1029/2005JD006341.

Moore, K. D., K. J. Voss, and H. R. Gordon (2000), Spectral reflectance of whitecaps: Their contribution to water-leaving radiance, *J. Geophys. Res.*, *105*, 6493–6499, doi:10.1029/1999JC900334.

Morys, M., F. M. Mims III, S. Hagerup, S. E. Anderson, A. Baker, J. Kia, and T. Walkup (2001), Design, calibration, and performance of MICROTOPS II handheld ozone monitor and Sun photometer, *J. Geophys. Res.*, *106*, 14,573–14,582, doi:10.1029/2001JD900103.

Porter, J. N., M. Miller, C. Pietras, and C. Motell (2001), Ship-based Sun photometer measurements using Microtops Sun photometers, *J. Atmos. Oceanic Technol.*, *18*, 765–774, doi:10.1175/1520-0426(2001)018<0765:SBSPMU>2.0.CO;2.

Quinn, P. K., D. J. Coffman, V. N. Kapustin, T. S. Bates, and D. S. Covert (1998), Aerosol optical properties in the marine boundary layer during the First Aerosol Characterization Experiment (ACE 1) and the underlying chemical and physical aerosol properties, *J. Geophys. Res.*, *103*, 16,547–16,563, doi:10.1029/97JD02345.

Remer, L. A., et al. (2002), Validation of MODIS aerosol retrieval over ocean, *Geophys. Res. Lett.*, *29*(12), 8008, doi:10.1029/2001GL013204.

Remer, L. A., et al. (2005), The MODIS aerosol algorithm, products, and validation, *J. Atmos. Sci.*, *62*, 947–973, doi:10.1175/JAS3385.1.

Remer, L. A., et al. (2008), Global aerosol climatology from the MODIS satellite sensors, *J. Geophys. Res.*, *113*, D14S07, doi:10.1029/2007JD009661.

Reynolds, R. M., D. Clark, E. Lettvin, and M. Schrader (2010), Around the Americas Expedition: Instrumenting a sailboat for science, *Sea Technol. Mag.*, *51*(8), 12–16.

Salomonson, V. V., W. L. Barnes, P. W. Maymon, H. E. Montgomery, and H. Ostrow (1989), MODIS: Advanced facility instrument for studies of the Earth as a system, *IEEE Trans. Geosci. Remote Sens.*, *27*, 145–153, doi:10.1109/36.20292.

Schuster, G. L., O. Dubovik, and B. N. Holben (2006), Ångström exponent and bimodal aerosol size distributions, *J. Geophys. Res.*, *111*, D07207, doi:10.1029/2005JD006328.

Shinozuka, Y., A. D. Clarke, S. G. Howell, V. N. Kapustin, and B. J. Huebert (2004), Sea-salt vertical profiles over the Southern and tropical Pacific oceans: Microphysics, optical properties, spatial variability, and variations with wind speed, *J. Geophys. Res.*, *109*, D24201, doi:10.1029/2004JD004975.

Smirnov, A., Y. Villevalde, N. O'Neill, A. Royer, and A. Tarussov (1995), Aerosol optical depth over the oceans: Analysis in terms of synoptic air mass types, *J. Geophys. Res.*, *100*, 16,639–16,650, doi:10.1029/95JD01265.

Smirnov, A., B. N. Holben, T. F. Eck, O. Dubovik, and I. Slutsker (2000a), Cloud-screening and quality control algorithms for the AERONET database, *Remote Sens. Environ.*, *73*, 337–349, doi:10.1016/S0034-4257(00)00109-7.

Smirnov, A., B. Holben, O. Dubovik, N. O'Neill, L. Remer, T. Eck, I. Slutsker, and D. Savoie (2000b), Measurement of atmospheric optical parameters on U.S. Atlantic coast sites, ships, and Bermuda during TARFOX, *J. Geophys. Res.*, *105*, 9887–9901, doi:10.1029/1999JD901067.

Smirnov, A., B. N. Holben, Y. J. Kaufman, O. Dubovik, T. F. Eck, I. Slutsker, C. Pietras, and R. Halthore (2002), Optical properties of atmospheric aerosol in maritime environments, *J. Atmos. Sci.*, *59*, 501–523, doi:10.1175/1520-0469(2002)059<0501:OPOAAI>2.0.CO;2.

Smirnov, A., B. N. Holben, T. F. Eck, O. Dubovik, and I. Slutsker (2003), Effect of wind speed on columnar aerosol optical properties at Midway Island, *J. Geophys. Res.*, *108*(D24), 4802, doi:10.1029/2003JD003879.

Smirnov, A., et al. (2009), Maritime Aerosol Network as a component of Aerosol Robotic Network, *J. Geophys. Res.*, *114*, D06204, doi:10.1029/2008JD011257.

Smirnov, A., et al. (2011), Maritime Aerosol Network as a component of AERONET—First results and comparison with global aerosol models and satellite retrievals, *Atmos. Meas. Tech. Discuss.*, *4*, 1–32, doi:10.5194/amtd-4-1-2011.

Tanré, D., Y. J. Kaufman, M. Herman, and S. Mattoo (1997), Remote sensing of aerosol properties over oceans using the MODIS/EOS spectral radiances, *J. Geophys. Res.*, *102*, 16,971–16,988, doi:10.1029/96JD03437.

Voss, K., E. Welton, P. Quinn, R. Frouin, M. Miller, and R. Reynolds (2001), Aerosol optical depth measurements during the Aerosols99 experiment, *J. Geophys. Res.*, *106*, 20,811–20,819, doi:10.1029/2000JD900783.

Zhang, J., and J. S. Reid (2006), MODIS aerosol product analysis for data assimilation: Assessment of over-ocean level 2 aerosol optical thickness retrievals, *J. Geophys. Res.*, *111*, D22207, doi:10.1029/2005JD006898.

Zhang, J., S. A. Christopher, L. A. Remer, and Y. J. Kaufman (2005), Shortwave aerosol radiative forcing over cloud-free oceans from Terra: 2. Seasonal and global distributions, *J. Geophys. Res.*, *110*, D10S24, doi:10.1029/2004JD005009.

T. P. Ackerman, A. F. Adames, and D. S. Covert, Joint Institute for the Study of the Atmosphere and Ocean, University of Washington, 408 ATG Bldg., Seattle, WA 98195, USA.

M. Reynolds, Remote Research and Measurement Company LLC, 214 Euclid Ave., Seattle, WA 98122-6528, USA.

A. Smirnov, NASA Goddard Space Flight Center, Bldg. 33, Rm. G406, Greenbelt, MD 20771, USA.